Received: 27 May 2022 | Revised: 30 June 2022 | Accepted: 2 July 2022

DOI: 10.1002/poc.4412

RESEARCH ARTICLE

Journal of Physical Organic Chemistry WILEY

Calculation of the relative basicity of three α,ω-diphenylpolyenes with trifluoroacetic acid

Mark B. Masthay[1] | **Jack B. McLean**[1] | **Ariana L. Santos**[1] | **Russell K. Pirlo**[2] | **Justin C. Biffinger**[1]

[1]Chemistry Department, University of Dayton, Dayton, OH, USA

[2]Chemical Engineering Department, University of Dayton, Dayton, OH, USA

Correspondence
Justin C. Biffinger, Chemistry Department, University of Dayton, 300 College Park, Dayton, OH 45469, USA.
Email: jbiffinger1@udayton.edu

Funding information
Ohio Action Fund; National Science Foundation, Grant/Award Number: CHE-2018678; UD Faculty Startup Funds; Strategic and Environmental Research and Development Program, Grant/Award Number: WP-1381

Abstract

Linear polyenes are an important class of compounds containing two or more alternating carbon-carbon double and single bonds that are soluble primarily in organic non-polar solvents. However, determining the relative basicity of unsubstituted polyenes experimentally has proven to be challenging in practice because such studies require mixing non-polar polyene-organic solvent mixtures with high concentrations of moderately polar organic acids. In this study, we used both computational and experimental approaches to calculate potential sites of protonation of *trans*-1,4-diphenyl-1,3-butadiene (DPB), all *trans*-1,6-diphenyl-1,3,5-hexatriene (DPH), and all *trans*-1,8-diphenyl-1,3,5,7-octatetraene (DPO) with trifluoroacetic acid (TFAH) in both *n*-hexane or benzene solvents. Density functional theory (DFT) calculations with a 6-311 + G (d,p) basis set and the B3LYP exchange correlation functional predict that the carbon atoms α to either phenyl ring are the most likely sites of protonation. Our calculations indicate that the basicities of the DPPs increase with increasing length of the polyene moiety (DPO > DPH >> DPB) in the gas phase and in both benzene and *n*-heptane solvents. Consistent with these computational predictions, the experimental rates of protonation of DPB, DPH, and DPO in benzene and hexane were consistent with the calculated basicity trends. Dynamic light scattering data confirmed that these reactions were phase separated resulting in emulsions between TFAH and both solvents; these phase separations complicated specification of the actual reaction rates. Finally, GC-MS and NMR data confirm that the crude products from the protonation of DPB and DPH were mixtures of DPB and DPH dimers. In significant contrast, DPO did not form dimers but rather an unidentified monomeric trifluoroacetate addition product.

SERDP WP-1381; University of Dayton STEM Catalyst Grant, University of Dayton Dean's Summer Fellowship; NSF MRI (CHE-2018678).

KEYWORDS
carbocation, polyene, polyene basicity, protonation

1 | INTRODUCTION

Linear polyenes constitute a broad category of both natural and purely synthetic molecules with many important and common subcategories.[1] "Pure" linear polyenes (C_nH_{n+2}), which belong to the C_{2h} point group, are synthetic hydrocarbons in which all of the carbon atoms are sp^2-hybridized. The carbon atoms are incorporated into linear conjugated arrangements of n C=C and (n–1) C–C bonds. Polyenes are present in photosynthetic systems[2] and play important antioxidant roles in biological systems involving free radicals (with tetraterpenoids),[3] and retinoids and carotenoids can thwart plant pathogen activity.[4] In addition, polyenes are weak, carbon π bases which protonate upon exposure to high concentrations of organic and inorganic acids in organic solvents resulting in carbocation intermediates.

One particularly important group of synthetically substituted linear polyenes is the α, ω–diphenylpolyenes (DPPs), which have terminal phenyl rings. DPPs are polarizable over the length of the conjugated system (like numerous other pure polyenes) and the polarizability results in large non-linear optical properties with potential applications in optical sensors or photorefractive crystals[5] or as imaging agents in the case of α,ω-di (4-pyridyl)polyenes.[6] In our recent study, to characterize the effectiveness of DPPs as acid sensitive probes in biodegrading polymer coatings,[7] *trans*-1,4-diphenyl-1,3-butadiene (DPB) and *all trans* 1,6-diphenyl-1,3,5-hexatriene (DPH) were chosen because of their commercial availability, their ease of use in molten polymers (DPB and DPH are low melting solids), and because DPPs are significantly more stable against oxidative degradation than retinoids and carotenoids. This makes DPPs interesting polymer additives for biodegradation research since they can be blended into non-polar polymer formulations, but the DPPs are not bioavailable to the microorganism degrading the polymers because when released they are not soluble in water. Thus, the irreversible color changes that occur when DPPs are protonated could potentially be mapped with a variety of spectroscopic techniques if the protonation reaction mechanism or products could be determined accurately.

The products resulting from the protonation of polyenes are theorized to be ion-paired complexes between the delocalized carbocation and the conjugate base of the acid. The existence of these ion-pairs was first proposed for carotenoids based on electrical conductance measurements.[8] More recently, variable temperature high-resolution NMR studies of protonated carotenoids[9] and retinoids[10] indicate that the colored protonation products are consistent with mono- and di-carbocation ion-paired intermediates. Multiple sites of protonation are possible with carotenoids (which contain 9 to 11 C=C bonds) and with retinoids (which contain five to six conjugated C=C bonds) because of the presence of methyl substituents throughout their conjugation pathways, resulting in stable, tertiary carbocation intermediates.

As is typical of conjugated pigments, the wavelength absorption maxima of linear polyenes increase with increasing numbers of C=C bonds. The protonation of linear polyenes results in large bathochromic shifts in their absorption spectra due to the delocalization of the positive charge in the resulting activated carbocations.[11] For example, retinoids turn blue upon reacting with the Lewis acid antimony trichloride in chloroform[11a] and β-carotene turns blue-green upon reacting with trifluoroacetic acid (a Brønsted acid) in benzene.[11c] A homologous series of α,ω-diphenylpolyenes turns a variety of colors upon reacting with tetrafluoroboric acid,[12] as does a series of homologous β,ψ-dimethyl polyenes upon reacting with sulfuric acid or tetrafluorobutyric acid.[13] For all of these species, the bathochromic shifts tend to be ∼10,000 cm^{-1} or greater in magnitude. Interestingly, and in direct contrast to the wavelength absorption maxima of unprotonated polyenes, the magnitude of the acid-induced bathochromic shifts does not depend strongly on the conjugation pathlength.[8,13]

Here, we report an experimental and computational comparison of the protonation of three different diphenyl polyenes (*trans*-1,4-diphenyl-1,3-butadiene [DPB] all *trans* -1,6-diphenyl-1,3,5-hexatriene [DPH] and *trans*-1,-8-diphenyl-1,3,5,7-octatetraene [DPO]) with neat trifluoroacetic acid (TFAH) in rigorously dried benzene or *n*-hexane. We used density functional theory calculations to predict the most likely site of protonation in the gas phase and with benzene or *n*-heptane solvent parameters. The relative basicity of all three DPPs were compared both in silico (via DFT calculations) and experimentally based on time dependent protonation-induced decreases in the intense UV absorption bands of the DPPs. To provide additional mechanistic and structural insights, we analyzed the crude products from the protonation of each DPP by UV-visible absorption, GC-MS, and qualitatively using ^1H and ^{19}F NMR spectroscopic methods.

2 | COMPUTATIONAL METHODS

$$DPP + TFAH \xrightleftharpoons{\Delta G_{rxn}} [DPP - H]^+ + TFA^- \quad (1)$$

Optimized geometries for all DPP structures were calculated using the *Gaussian* 16 software package (*Gaussian 16*, Revision C.01,[14] with *Gaussview* 6[15]). We used the DFT method with a 6-311 + G (d,p) basis set and B3LYP exchange correlation functional with a tight convergence criterion for all frequency and geometry optimization calculations. All full geometry optimizations were found to be true minima with zero imaginary frequencies. The calculation of the gas phase basicity was determined using the corresponding sums and differences of the electronic and thermal free energy correction values resulting from the DFT frequency calculations.[16] Every thermodynamic value from these calculations can be found in the supporting information, and the optimized geometries atomic coordinates of all acids, anions, and DPPs presented in this work are available on request.

The ground state energies of the various potential protonation sites (see Figure 1) were calculated for each carbocation $[DPP\text{-}H]^+$ (i.e., protonated DPPs) to calculate the relative basicity of each compound using Equation 1 in the gas phase. Building upon the gas phase results, we performed frequency/optimization calculations on only the α-protonated carbocations (which our calculations indicated were the most stable of the possible carbocations) with either benzene or *n*-heptane solvent parameters using a continuous level Monte Carlo (CLMC) approach.[17]

3 | RESULTS AND DISCUSSION

3.1 | Predicting the protonation site of DPPs

There are several potential sites of protonation along the linear conjugated region of the DPPs used in this study; each potential site is labeled in Figure 1 relative to the terminal phenyl rings. Depending on the protonation site and the length of the conjugation pathway, both localized benzylic carbocations and benzylic carbocations delocalized across the full length of the polyene are possible. These three DPPs have shorter unsubstituted conjugation structures than retinoids and carotenoids, which makes multiple protonation unlikely due to electrostatic effects.[9b,11c] Thus, we only considered monoprotonated species for all calculations.

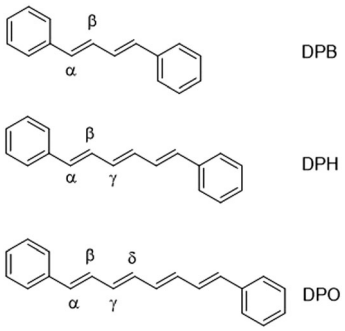

FIGURE 1 Structures of the DPPs used in these experiments and the labeling for the sites of protonation

We exclusively utilized trifluoroacetic acid (TFAH) to protonate the DPPs in these experiments and calculations, for four reasons: (1) TFAH is a strong enough acid to protonate bases as weak as these DPPs; (2) the polarity of TFAH is small enough that it has a high solubility in non-polar organic solvents; (3) TFAH is stable enough to not generate undesirable side products (unlike trichloroacetic acid which is predicted to decompose into various chlorine-containing species during general acid catalysis conditions)[18]; and (4) because TFAH has been used successfully to study solvolysis reaction mechanisms.[19] Consequently, TFAH is a stable and strong organic acid for use in organic media.[20]

The geometry-optimized structures of the parent polyenes and all potential carbocation intermediates were generated using DFT ground state optimization/frequency calculations. We compared the ground state energies of all protonated polyenes at the α, β sites (for DPB, DPH, DPO), γ sites (for DPH and DPO), and the δ site (for DPO only). The electronic energies accounting for thermal Gibb's free energy corrections were used to calculate the free energy change for protonation[16] in the gas phase which is a measure of the equilibrium constant for protonating each polyene at the designated site (Table 1). The gas phase basicity of the α protonated intermediate for DPB, DPH, and DPO were 8.0, 10.6, and 13 kcal/mol more basic than the β-protonated sites, respectively. The differences between the basicity of β and γ protonated for both DPH and DPO and the γ and δ protonated DPO were significantly smaller than those between the α and β protonated species (i.e., $\Delta E_{\alpha\beta} > \Delta E_{\gamma\delta} > \Delta E_{\beta\gamma}$). These data thus predict that the most basic site on these DPPs is α to one of the phenyl rings for all three DPPs. In this regard, it is noteworthy that protonation at the α sites also maximizes the extent of the delocalization of the resulting benzylic carbocations in DPPs.

In similar fashion, "pure" polyenes C_nH_{2n+2}, which lack the terminal phenyl rings, are expected to protonate at the terminal carbon atoms, resulting in maximally

TABLE 1 Results from DFT[a] calculations of ground state energies of protonated and unprotonated DPPs and the results of gas phase basicity calculations from the protonation at the designated sites (Figure 1)

Compound	Electronic energy (EE)[b]	EE + Gc_{orr}[b]	ΔG_{rxn} (kcal/mol)	K[c]
DPB	−618.2744	−618.0699	-	-
DPB (α H^+)	−618.6247	−618.4081	106	3×10^{-78}
DPB (β H^+)	−618.6128	−618.3949	114	2×10^{-84}
DPH	−695.7022	−695.4677	-	-
DPH (α H^+)	−696.0644	−695.8180	98.4	8×10^{-73}
DPH (β H^+)	−696.0490	−695.8007	109	1×10^{-80}
DPH (γ H^+)	−696.0496	−695.8028	108	1×10^{-79}
DPO	−773.1301	−772.8659	-	-
DPO (α H^+)	−773.5015	−773.2249	93	1×10^{-68}
DPO (β H^+)	−773.4820	−773.2038	106	2×10^{-78}
DPO (γ H^+)	−773.4875	−773.2112	106	3×10^{-78}
DPO (δ H^+)	−773.4812	−773.2042	101	5×10^{-75}
TFAH	−526.9660	−526.9582	-	-
TFA^-	−526.4448	−526.4514	-	-

[a]6-311 + G(d,p) basis set with B3LYP hybrid electron correlation functional. Temperature = 298.15 K, G_{Corr} = Thermal Free Energy Correction and Gibb's Free Energy change of reaction in Equation (1) ΔG_{rxn}.
[b]Values are in Hartrees.
[c]$K = e^{-\frac{\Delta G_{rxn}}{RT}}$, $\Delta G_{rxn} = \sum(EE + G_{corr})_{products} - \sum(EE + G_{corr})_{reactants}$.

delocalized 2° carbocations. Naturally occurring C_{40}-carotenoids like β-carotene (βC), which are terpenoids, have six methyl substituents spaced five carbons apart at the 5, 9, 13, 13′, 9 ′, and 5 ′ positions along their polyene chains. As a result, carotenoids undergo in-chain protonation,[9a,b,11c] which facilitates the generation of especially stable 3° carbocations at the methylated positions, in addition to maximizing the extent of carbocation delocalization. Consistent with these factors,[21] experimental results indicate that βC,[22] lycopene,[23] and astaxanthin[24] have K_b values of 0.4 ± 0.1, 0.5 ± 0.1, and 0.4 ± 0.1, respectively, with trichloroacetic acid in benzene solvent. Hence, carotenoids are much stronger carbon π-bases than the DPPs. It is also noteworthy as well that carotenoids undergo double protonation in the presence of molar excess of acid.[11c,22]

3.2 | DFT calculations of the relative basicity of DPPs in non-polar organic solvents with TFAH

The gas phase calculations confirmed that the most likely site of protonation is α to the phenyl rings for all DPPs. Hence, we used the ground state energies of all α protonated intermediates ($[DPP\text{-}H]^+$), trifluoroacetic acid (TFAH), trifluoroacetate (TFA^-), and the parent DPP with continuous level Monte Carlo (CLMC) methods with solvent parameters for benzene or *n*-heptane to calculate the Gibb's Free Energy Change and the basicity constant (K) for the equilibrium shown in Equation 1. CLMC methods were use because they reduce computational costs by using coarse-scale models with lower fidelity for bulk solvent simulations, while at the same time maintaining the precision of the optimized structures from the molecular geometry calculation.[17]

The results from the calculation of the basicities from the electronic energies corrected with Thermal Gibb's Free Energy values of DPB, DPH, and DPO in each solvent are shown in Table 2. This table summarizes the results of these calculations including the calculation of the qualitative equilibrium constants (K). The thermodynamic values used to calculate ΔG_{rxn} can be found in the supporting information. The results from these calculations are consistent with the gas phase basicity trends: K (DPO) > K (DPH) >> K (DPB). It is noteworthy that, while the K values of all three compounds are very small in the gas phase, the addition of solvent causes the values of both K (DPH) and K (DPO) to increase by ∼35 and ∼28 orders of magnitude in benzene and *n*-heptane, respectively, while leaving the value of K (DPB) relatively unchanged from its gas phase value. It is likely that these nonpolar solvents preferentially stabilize isolated protonated DPPs with longer conjugation pathways ($DPHH^+$ and $DPOH^+$) or their respective contact ion pairs

(DPHH$^+$···TFA$^-$ and DPOH$^+$···TFA$^-$) as compared to those with shorter conjugation pathways (DPBH$^+$ and DPBH$^+$···TFA$^-$).

These calculations also predict that DPPs are more basic in an aromatic solvent (benzene) than a saturated alkane solvent (i.e., *n*-heptane) presumably because the π-delocalized carbocations can be stabilized by interactions with the polarizable π-clouds of benzene. That said, we are not certain the CLMC method is sensitive to this level of molecular detail, but the results suggest this trend is possible. The largest difference in basicity was calculated to be between DPB and DPO in *n*-heptane ($K_{(DPO)}/K_{(DPB)} = 7 \times 10^{44}$) and this difference is borne out in our experimental results (see below).

To date, the basicity of DPB and DPH have only been reported in the gas phase using semi-empirical ZINDO level calculations with published thermodynamic values for the gas phase proton.[7] In direct contradiction to the calculated basicities in the current work, these previous gas phase-only calculations suggested that DPB is a stronger base than DPH. There are two potential reasons why our earlier ZINDO results were flawed. First, and most importantly, the calculation of the basicity of DPB and DPH in the ZINDO calculations did not account for the contributions from the TFAH, TFA$^-$, and the solvent, but rather corresponded to calculations of ΔG for "proton affinity." Second, ZINDO can overestimate the contribution of π-bonding, and consequently might have led to errors in the relative ground state energies based on disrupting the highly conjugated polyene moieties upon protonation. The choice of DFT methods, inclusion of DPO, and the extended basis set in this current work addresses these earlier potential computational concerns.

3.3 | Experimental results for the protonation of DPPs in non-polar organic solvents with Trifluoroacetic acid

The calculations reported in Table 2 predict that DPO and DPH are significantly stronger bases than DPB. To test the qualitative reliability of these computational results, we attempted to calculate the experimental basicity of these DPPs using high concentrations of TFAH in either benzene or *n*-hexane. In earlier studies of the highly colored products generated from the reactions of retinoids and carotenoids with both Brønsted (trifluoroacetic[9b,11c] and trichloroacetic[8,25] acids) and Lewis ($SbCl_3$[26] and BF_3-etherate[10]) acids suggested that carbocation ion-paired complexes and/or polyene-acid adducts were generated. For example, solutions of the orange carotenoid β–carotene ($\lambda_{max} \sim 450$ nm, 11 C=C bonds) dissolved in a variety of organic solvents manifest large (≥+350 nm, ~9,700 cm^{-1}) bathochromic shifts upon the addition of large molar excesses of TFAH.[10,11c,25] The resulting blue green species typically manifest absorption maxima at wavelengths ≥900 nm at [TFAH]/[β-carotene] ratios of 50,000 or higher.[11c] Retinoids ($\lambda_{max} \sim 300$–360 nm, 5–6 C=C bonds) manifest similar color changes, most famously via the Carr-Price color reaction with $SbCl_3$, which results in blue complexes with absorption maxima in the 600–700 nm range (>10,000 cm^{-1} bathochromic shifts).[26] Somewhat surprisingly, α,ω-diphenyl polyenes[12] and β,ψ-dimethylpolyenes manifest bathochromic shifts of similar magnitude (~10,000 cm^{-1}) regardless of their conjugation pathlengths. The final colors of these protonated species thus depend on the λ_{max} values of their unprotonated parent compounds.

TABLE 2 Results from the DFT[a] basicity calculation of α protonated DPPs including CLCM solvent parameters for benzene and *n*-heptane

	Benzene		
Compound	**ΔG_{rxn} (Hartree)**	**ΔG_{rxn} (kcal/mol)**	**K[b]**
DPB	0.1655	103.9	7×10^{-77}
DPH	0.0817	51.3	3×10^{-38}
DPO	0.0752	47.1	3×10^{-35}
	***n*-Heptane**		
Compound	**ΔG_{rxn} (Hartree)**	**ΔG_{rxn} (kcal/mol)**	**K[b]**
DPB	0.1836	115.2	3×10^{-85}
DPH	0.0935	58.7	1×10^{-44}
DPO	0.0863	54.2	2×10^{-40}

[a]6-311 + G(d,p) basis set with B3LYP hybrid electron correlation functional. Temperature = 298.15 K.
[b]$K = e^{-\frac{\Delta G_{rxn}}{RT}}$, $\Delta G_{rxn} = \sum(EE + Gcorr)_{products} - \sum(EE + Gcorr)_{reactants}$. All calculated thermodynamic energy values can be found in the supporting information.

We used the change in concentration of each DPP over time to calculate the rate of the protonation reaction using the change in the absorbance from the strongly absorbing UV bands of the parent DPP below 400 nm (Figure 2). For these DPPs, the absorbances attributed to $\pi \rightarrow \pi^*$ transitions occur in the 250–400 nm range. To limit potential side reactions of our acid-DPP complexes, we performed the protonation reactions in rigorously dried and air-free benzene or *n*-hexane. The DPPs were reacted at concentrations of 1.7×10^{-5} M in either 0.039, 3.9, or 9.7 M TFAH (corresponding to 1,950, 195,000, and 495,000 molar excess of TFAH to DPP, respectively) in either benzene or *n*-hexane. Figure 2 shows the spectra collected initially, after 500 min, and after 2,000 min from the reaction of each DPP with 3.9 M TFAH. Figure 2 insets are the spectra of the colored products between 400 and 800 nm. The spectra for the 9.7 M TFAH experiments in both solvents were identical to the 3.9 M experiments (data not shown).

In spite of our numerous attempts to observe an equilibrium between TFAH and the resulting protonated carbocation, the lack of isosbestic behavior in our spectral data confirmed that a single protonated product was not generated at 3.9×10^{-2}, 3.9, and 9.7 M TFAH in either solvent. For DPB and DPH, a new absorbance between 400 and 650 nm increased over time, but only in benzene. However, the spectroscopic changes observed for DPB and DPH above 400 nm (in benzene only) were unlike what was observed with DPO. For DPO, an intermediate with a λ_{max} of 667 nm (Figure 2C, inset) was observed ~ 500 min after the reaction was initiated. Subsequently, this blue-colored species underwent a hypsochromic shift, yielding a final product with a $\lambda_{max} < 610$ nm at 2000 min. It is noteworthy that the temporal changes in the spectrum of the DPO intermediate are in some ways similar to those of β-carotene–TFAH intermediates in benzene.[11a] These spectroscopic data are consistent with the formation of several different compounds terminated with either residual nucleophiles[27] or dimerization and not products that result from protonations.[9b,11c]

The kinetics of these reactions was complicated spectroscopically. Increasing the concentration of TFAH 100-fold from 0.039 to 3.9 M increased the initial rate of reaction by over 10,000-fold, thus suggesting an approximately quadratic dependence on concentration of TFAH. Mortensen and Skibsted [11c] reported a similar quadratic increase in rate when protonating β-carotene with TFAH. Increasing the concentration of TFAH from 3.9 to 9.7 M did not change the initial rate of disappearance of DPB, DPH, nor DPO. This zeroth-order dependence on [TFAH] at the highest concentrations tested suggests that some other factor is affecting the observed rates of reaction. However, the initial rates of disappearance of DPB (5.3×10^{-8} M min^{-1}), DPH (1.5×10^{-7} M min^{-1}) and

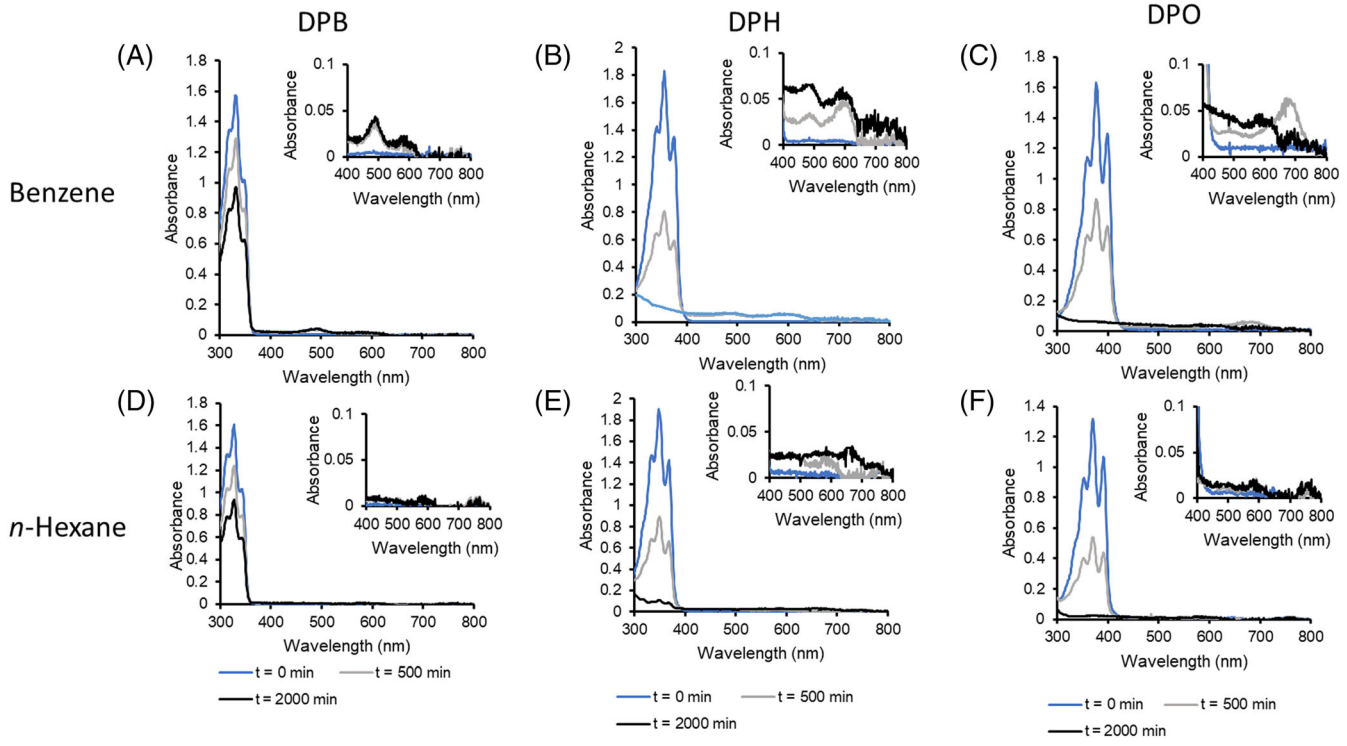

FIGURE 2 Absorption spectra of DPB (A (Benzene), D (*n*-Hexane)), DPH (B (Benzene), E (*n*-Hexane)), and DPO (C (Benzene), F (*n*-Hexane)) 0, 500, and 2,000 min after mixing with 3.9 M Trifluoroacetic acid. Figure insets: UV-visible absorption spectra highlighting the absorbance changes that occurred between 400 and 800 nm

DPO (2.5×10^{-7} M min^{-1}) in benzene with 3.9 M TFAH indicate that the observed relative rates of disappearance of the unprotonated DPPs agree with our calculated basicities (Table 1), which also increase with increasing polyene chain length. This conclusion is predicated on the rate determining step being the initial protonation step as is typically observed for alkenes in general.[28] The initial rates of disappearance of all DPPs were four-fold slower in *n*-hexane compared to benzene at 3.9 M TFAH. This result is also consistent with the computational thermodynamic results in Table 1, which indicate that all DPPs are less basic in *n*-heptane than in benzene. The final products which formed in *n*-hexane did not have high molar absorptivities in the visible region of the electromagnetic spectrum, in distinct contrast to the products which formed in benzene (Figure 2).

Aside from the fact that the DPB reaction was 13 times faster in benzene (5.3×10^{-8} M/s) than in *n*-hexane (4.1×10^{-9} M/s), there was no significant change in the reactivity patterns of these DPPs in *n*-hexane. These data are consistent with our computational results, which also indicated that all three DPPs are stronger bases in aromatic solvents than in linear saturated alkane solvents. It is noteworthy that the colored species are generated only in benzene and not *n*-hexane. The structural differences between these protonated products in aromatic and alkane solvents is being actively pursued by our group. For now, we speculate that the difference between the solvents for the protonation of DPPs could be due to stabilization of post-protonation $DPPH^{+}$–TFA^{--} contact ion pairs and/or DPP–TFAH adducts with the polarizable electronic π–clouds of benzene.

These spectroscopic and kinetic results could also be attributed to the "Winstein ion-pair mechanism," a salt effect which is operative during protonation reactions generating carbocations.[20b,29] However, considering the disparate polarities of the non-polar solvents and the organic acids used for these reactions, there is another more reasonable explanation for the complicated kinetics observed from these reactions. The differences between the absorption spectra shown in Figure 2A–C in benzene and Figure 2E,F in *n*-hexane could potentially originate from the formation of TFAH-solvent (or TFAH-DPP-solvent) emulsions that occur when mixing nonpolar solvents with high concentrations of TFAH (dipole moment: 2.21 Debyes). The separation into two phases can create mass-transfer related dynamics between the phases, resulting in complicated kinetic data sets.[30] It is significant, then, emulsion formation in reactions similar to ours has been explored only minimally by other researchers[10] in spite of the high concentrations of TFAH used in these other studies.[20b]

Accordingly, we performed dynamic light scattering (DLS) measurements to determine if emulsions were formed in our experiments. The light scattering data from the DLS measurements of the solvent-TFAH-DPP mixtures are shown in Figure S2. The maximum "particle" sizes, including standard deviation of the maximum "particle" size, are detailed in Table 3. These data confirm the presence of emulsions at TFAH concentrations greater than 3.9 M TFAH in "blank" (i.e., no DPP present) solutions since nanometer sized droplets were observed in both benzene: TFAH and *n*-hexane: TFAH solutions for [TFAH] = 3.9 M. In contrast, 100- to 1,000-fold increases in droplet size (>1–2 μm) droplets were observed for [TFAH] = 9.7 M mixtures with DPH and DPO in benzene and with DPO in *n*-hexane. These differences in droplet size are significant since, assuming ideal solutions, TFAH is expected to act as the solvent, since [TFAH] > [benzene] and [*n*-hexane] at 9.7 M.

DLS measurements revealed no phase separations in "blank" 0.039 M TFAH solutions (Figure S1) but did reveal phase separations in "blank" 3.9 and 9.7 M TFAH solutions, confirming that droplet size increased with increasing TFAH concentration with no DPP present. Significantly, we also did not observe the protonation of any DPP at 0.039 M TFAH, suggesting that solvent-TFAH phase interface in emulsions strongly facilitates the reaction of TFAH with DPPs. That is, our results suggest that the protonation of DPPs is not only dependent upon TFAH concentration at low concentrations but on the TFAH/solvent concentration ratio.

The trends in the DLS data from the reaction with DPB, DPH, and DPO with 3.9 M TFAH in benzene showed that the droplet size decreases with increasing polyene chain length and basicity (Table 3). These same measurements at 9.7 M TFAH in benzene showed the exact opposite size dependence trend and resulted in much larger droplets. However, it is notable that the actual raw data from these measurements (Figure S2) show significantly different polydispersity of these emulsions. Even so, the formation of these emulsions should not affect the relative comparisons we present in this current work since the reaction conditions were uniform across the experiments and compounds. Most importantly, *our results clearly demonstrate the necessity of emulsion droplets for protonation*, as the protonation of DPB and DPH does not occur for DPB and DPH in neat TFAH over 2 months (data not shown). It is interesting to note in this regard that historically very large concentrations of TFAH have been used in studies of the effect of acids on carotenoids, though with rare exception,[9b,c] the possibility of emulsions and their potential impact on protonation reactions was not discussed.

TABLE 3 Dynamic light scattering data from solutions of benzene or *n*-hexane with 0.039, 3.9, or 9.7 M trifluoroacetic acid ("blank" solutions) or from the end of the reaction with DPB, DPH, or DPO present

Compound	Maximum "particle" diameter (nm) 0.039 M TFAH	Maximum "particle" diameter (nm) 3.9 M TFAH	Maximum "particle" diameter (nm) 9.7 M TFAH
Solvent: Benzene			
DPB	-	1.81 ± 0.52	214 ± 148
DPH	-	1.72 ± 0.41	1980 ± 154
DPO	-	0.55 ± 0.16	2,430 ± 142
Blank	-	1.79 ± 0.51	201 ± 89
Solvent: *n*-hexane			
DPB	-	2.14 ± 0.99	127 ± 33
DPH	-	0.52 ± 0.16	153 ± 64
DPO	-	1.78 ± 0.75	1970 ± 111
Blank	-	2.03 ± 0.77	115 ± 41

Although the appearance of colored protonated polyenes has been ascribed to ion pairing between the carbocation intermediate and the conjugate base of the acid,[20b] our results indicate that the reaction of DPO with TFAH was consistent with the formation of a long-lived ion-paired intermediate. Hafner and Pelster first reported ion pairing in mixtures of diphenylpolyenes and HBF_4 in ether in 1961. However, these authors did not present evidence for the structures of the actual products, just the colors.[12] Subsequently, in 1965, Sorensen[13] reported NMR resonances and electronic spectra of blue species consistent with intramolecularly-rearranged products resulting from the protonation of tetraenes, pentaenes, and hexaenes in 96% sulfuric acid. The use of 96% sulfuric acid in Sorensen's experiments resulted not only in intramolecularly-rearranged cyclized carbocation products, but also in alcohols and other oxidized side products resulting (most likely) from the presence of water and oxygen in their experiments. Under our dry, anaerobic reaction conditions, potential side reactions with water were minimized but certainly intramolecular-rearranged products would be possible with these DPPs.

3.4 | Preliminary identification of the products from the reaction of Trifluoroacetic acid with DPPs

Since the absorption spectra for DPB, DPH, and DPO in benzene confirmed that stable, colored products were generated instead of protonated carbocation intermediates in equilibrium with the parent DPP, we can only estimate the relative basicity of these DPPs from the rate of disappearance of the unprotonated DPP. To elucidate the possible subsequent reactions after protonation, as well as the structures of the final, stable colored products, we analyzed the crude product mixtures from these reactions directly by gas chromatography with mass spectroscopic detection (GC-MS) and ^{1}H or ^{19}F NMR spectroscopy. Briefly, we vacuum transferred the solvents and unreacted DPPs, the latter of which readily sublime at room temperature, leaving behind the colored crude product at the end of the reaction. The crude product was then placed on a Schlenk vacuum line for 24 h at room temperature to remove any residual reagent. Then, each crude product was dissolved in either methylene chloride for GC-MS measurements or $CDCl_3$ for NMR measurements.

The gas chromatographic separations of the crude DPB, DPH, and DPO reaction products from 3.9 M TFAH in benzene are shown in Figure 3. The EI MS spectra of the major products in these crude reaction mixtures are shown in the color-matched inset figures. The gas chromatographic separation confirmed that the crude reaction mixtures for DPB, DPH, and DPO each contained one primary product which was unique to each DPP. In addition, the product mixtures for DPB, DPH, and DPO contained 12, 8, and 5 additional minor products, respectively. All of these additional products had longer retention times than the major products, suggesting that they were either more polar, of higher molecular weight, or both as compared to the major products.

The major and minor products from the protonation of DPB and DPH were the result of dimerization. The molecular ion peak in the mass spectra of the major product (45% of the total area of peaks in the crude mixture) from the protonation of DPB with TFAH was 412.5 *m/z* (Figure 2, orange inset) which corresponds to the mass of a DPB dimer. This same mass was observed for the molecular ion peak of 90% of the other 12 products

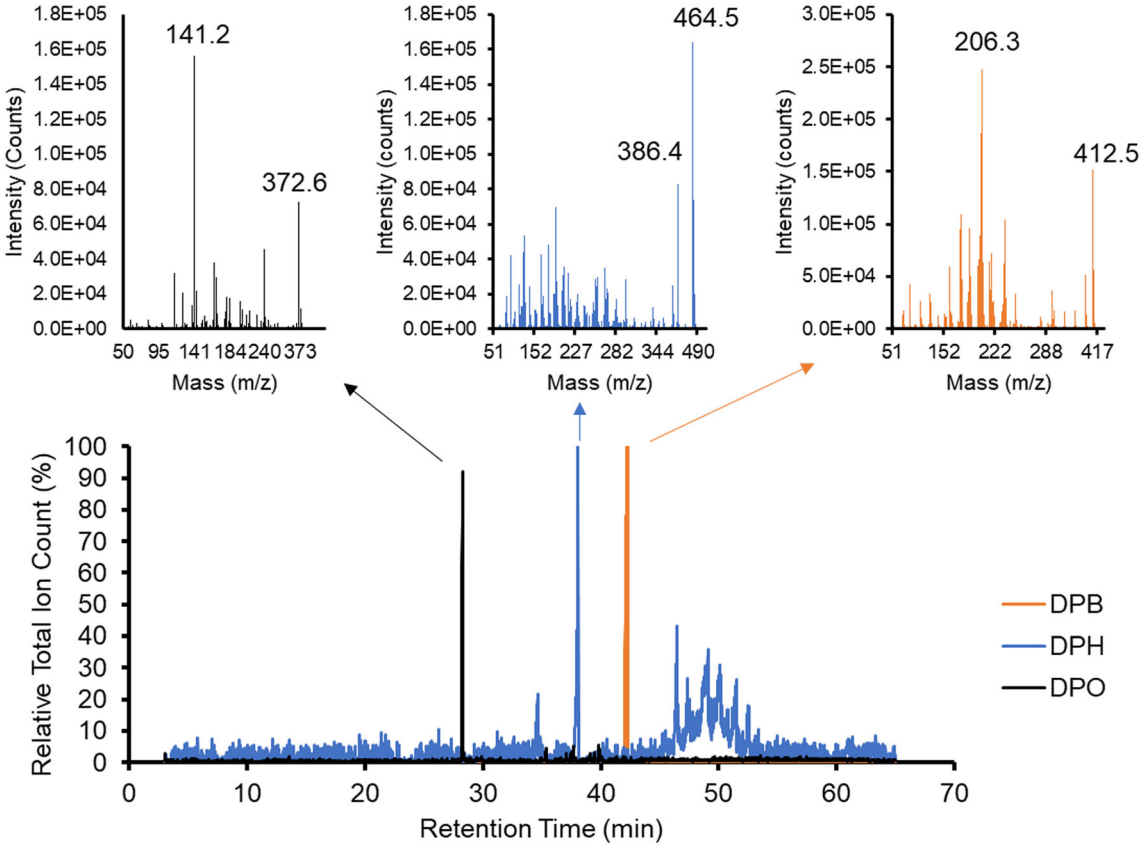

FIGURE 3 GC-MS chromatograms of the crude product after the protonation of DPB, DPH, and DPO with trifluoroacetic acid (3.9 M) in benzene. Electron impact mass spectra are shown in the insets for the major product in each chromatogram

in the crude DPB product mixture. The first mass loss was 78 *m/z*, indicating the loss of a benzene ring with a proton which is consistent with the original DPB structure. The base peak of the mass spectrum was 206.4 *m/z* which is consistent with the mass of one $DPBH^+$ fragment. Similarly, the molecular ion peak of the major DPH protonated product was 464.5 m/z (Figure 3, blue inset) and is also consistent with the mass of a DPH dimer. This same molecular ion peak was observed for the other 8 products in the crude DPH product mixture. The first mass loss (and base peak of 386.4 *m/z*) of the primary product was 78 *m/z* and is indicative of the loss of a phenyl and proton cation from the parent compound.

These protonated dimeric products could be any manner of linear or cyclic structure. The cyclization of polyenes with Lewis acids was first reported by Stork and Burgstalhler[31] in 1955 with 1,5-dienes. Numerous cyclized compounds containing fused polycyclic rings[32] or simple alkenyl alcohols[33] were observed for similar reactions previously. The predominance of cyclic alkyl structures in our experiments is also supported by the chemical shifts of the resonances in the crude ^{1}H NMRs for DPB (Figure S3**)** and DPH (Figure S4). These NMRs show that not only was there no residual unprotonated starting material but several new ^{1}H resonances in the crude product mixture consistent with hydrogens on sp^3 hybridized carbons (below 2.5 ppm), consistent with resonances expected from mixtures of cycloalkene-based structures with 4, 5, 6, 7 carbon rings or potentially bicyclic cycloalkenes.[33a,34] We are currently pursuing scaled up reactions to isolate and purify these compounds individually. Even so, the data we present here clearly indicate that the colored products generated from the protonation of DPB and DPH are cyclized dimers from either DPB or DPH.

Throughout these protonation experiments, the reactivity of DPO with TFAH was significantly different than that of DPB and DPH, both in terms of the spectroscopy and the final observed products. We hypothesize that the differences in the reactivity of DPO compared to DPB and DPH are attributed to the increasing stability of the delocalized carbocation intermediate as the conjugated chain is extended as was observed from our computational data. Mechanistically, an intermediate species was only observed (λ_{max} = 675 nm) within 500 min after adding the TFAH to a benzene–DPO mixture (Figure 2C) and not DPB nor DPH. This intermediate decayed over

the subsequent 1,500 min to a more weakly absorbing $\lambda_{max} \sim 610$ nm species which was the crude protonated product analyzed by GC-MS and NMR. The GC-MS chromatogram showed that 90% of the crude product was a single compound that eluted at 28.3 min (Figure 3, black trace and inset). The molecular ion peak of this product was 372.6 *m/z* and a base peak of 141.2 *m/z*. The molecular ion peak is consistent with a $DPOH^+$, trifluoroacetate ion pair ($CF_3CO_2^-$) and not a dimer like the products observed from the protonation of DPB or DPH. The base peak at 141.2 *m/z* is most likely from the fragmentation of the $DPOH^+$ cation. The ^1H NMR of this crude product is also consistent with a breaking of the symmetry of the DPO structure because of the magnetic inequivalence observed in the ^1H NMR resonances between 7.5-8.5 ppm for the phenyl rings (Figure S5) compared to the unprotonated DPO.

The presence of trifluoroacetate within this crude DPO product is also supported by the comparison of the ^{19}F NMR spectra of the crude product mixtures for of all three DPPs (Figure 4). These data confirm that ^{19}F NMR signals are observed only for the DPO crude product and not DPB nor DPH. The two ^{19}F NMR resonances observed for the DPOH–$CF_3CO_2^-$ products occur at −75.8 ppm and −74.6 ppm, indicating that there were two significantly different trifluoromethyl environments in the crude product. Based on earlier studies of TFAH adducts to similar compounds,[35] the more upfield ^{19}F resonance is consistent with a $DPOH^+$ ... $CF_3CO_2^-$ contact ion pair species and the more downfield resonance is consistent with covalently–bonded DPO–CF_3CO_2 adduct. The formation of contact ion pairs or adducts is also consistent with the products observed from reactions of substituted styrenes,[36] 3–methyl–1–butene,[20a] and to 1–octene[37] with TFAH.

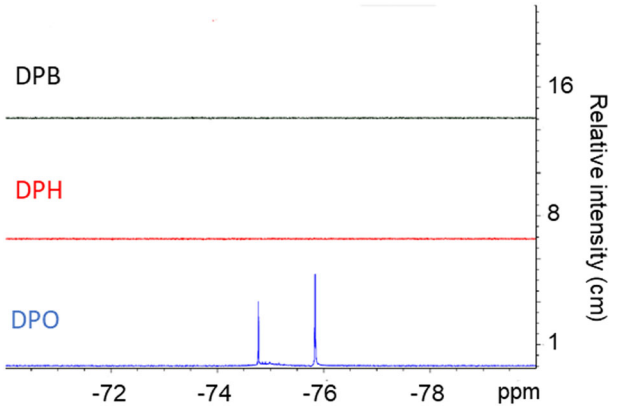

FIGURE 4 Comparison of the ^{19}F NMR (376 MHz, $CDCl_3$) spectra for the crude products from the protonation of DPB, DPH, and DPO with 3.9 M trifluoroacetic acid in benzene

Collectively, the relative stability of the initial contact ion pairs, the subsequent adducts, and other subsequent side products precluded the generation of accurate experimental estimates of the absolute basicities (K values) of DPB, DPH, and DPO. Hence, we were relegated to using the relative initial rate constants for the reactions of DPB, DPH, and DPO with TFAH to estimate the relative basicity trend. Regardless, it is clear that the relative basicity trend, both computationally and experimentally, follows the trend DPO > DPH >> DPB even though the end products for DPB and DBH clearly differed from DPO.

4 | CONCLUSIONS

In summary, our calculations support that (1) α,ω-diphenylpolyenes preferentially protonate at the carbon atoms α to the phenyl rings. (2) The colored protonated products were primarily dimers of DPB and DPH and a monomeric trifluoroacetate adduct of protonated DPO. (3) The basicity of the DPPs in this study increased with the increasing length of conjugation resulting in K (DPO) > K (DPH) >> K (DPB) as confirmed using both DFT computations and comparisons of initial rates of disappearance of each DPP protonated with TFAH. (4) DLS data confirmed that the use of high concentrations (≥3.9 M) of TFAH in the non-polar solvents chosen for these experiments creates emulsions in which the solvent-TFAH interface most likely facilitates the protonation of DPPs and complicate the kinetic measurements.

DPPs are predicted to be very weak bases in both benzene and *n*-hexane considering our calculation of the basicity of the strongest base (DPO) in this series of polyenes has a small magnitude of $K = 1 \times 10^{-35}$ (in benzene). In this regard, it is important to note that the DFT calculations accurately predict *trends* in basicity, but not *absolute values* for K. In addition, there were several other factors that circumvented the accurate calculation of these basicities spectroscopically including the presence of emulsions and the subsequent reactivity of the carbocation intermediates resulting in no isosbestic points in the spectra.

DPPs constitute a unique class of colorimetric weak bases for imaging acid gradients developing in non-polar polymers since the inherent reactivity of the DPP carbocation intermediates terminates with either colored dimerized products (DPB or DPH) or colored contact ion pairs or adducts (DPO). These compounds cannot be regarded as acid-base indicators in the classical sense, as our experiments indicate that the initial protonation of the reactions for the three DPPs are not reversible. In analogy with the strongly basic carotenoid, β-carotene, it

is likely that methylation of DPPs at various positions along their polyene conjugation pathways may make them stronger bases and potentially prevent the dimerization of these compounds. Hence, methylated DPPs may be more effective acid front indicators than unsubstituted DPPs.

5 | EXPERIMENTAL METHODS

5.1 | Materials

All *trans* 1,6-Diphenyl-1,3,5-hexatriene (98%), all *trans*-1,-4-diphenyl-1,3-butadiene (98%), and 1,8-diphenyl-1,3,5,7-octatetraene were purchased from Sigma Aldrich and used as received. Benzene was purchased from Fisher Scientific, dried over CaH_2 and vacuum distilled. *n*-Hexane (Fisher) was distilled from sodium metal, and the latter fraction was dried over 4 Å molecular sieves. Trifluoroacetic acid (95%) was purchased from Sigma Aldrich, dried over P_2O_5 and vacuum distilled with partial freezing into an air-free storage tube prior to use.

5.2 | Protonation of diphenyl polyenes in organic solvents (spectroscopic determination) with trifluoroacetic acid (TFAH) and the characterization of the crude reaction mixtures

Each DPP was added to a 10 ml volumetric flask and dissolved to a final concentration of 2×10^{-5} M in either dry benzene or dry *n*-hexane. TFAH was added to both solvents to create solutions with final TFAH concentrations of 3.9×10^{-2}, 3.9, and 9.7 M. The reactions were observed spectroscopically over 48 h at 25°C unless otherwise indicated. The absorption spectra of the resulting solutions were then acquired periodically throughout the experiment with a Hewlett Packard 8453A UV-visible spectrophotometer and 1 cm PTFE sealed quartz cuvettes. The solvent, unreacted DPPs, and TFAH were then vacuum transferred from the highly colored products. The remaining product residues were dissolved in chloroform and analyzed by GC-MS using a Trace 1310 Gas-Chromatography System with an ISQ 7000 Single Quadrupole Mass Spectroscopy detector using Electron Impact (EI) Ionization (70 eV, source temperature 200°C). Samples were injected directly onto a 30 m Rtx®5-MS capillary column (Restek) using a splitless injection and He carrier gas. The injector temperature was 250°C. The separations were performed using a gradient temperature program (100°C [hold for 2 min] then a slow 5°C/min temperature gradient to 300°C [held 5 min]). A mass range (m/z) of 50–800 was acquired. The products from the fractions were also analyzed by ^{1}H and ^{19}F NMR on a 400 MHz Bruker Spectrophotometer in *d*-chloroform. All experiments were performed in duplicate with the data from one set of replicates presented in this manuscript.

5.3 | Particle size measurements of trifluoroacetic acid solutions with *n*-hexane or benzene

Dynamic light scattering (DLS) spectra were collected to confirm the presence of emulsions using a Litesizer 500 (Anton-Paar, UK) particle size analyzer in quartz cuvettes (Anton Parr, UK) at 25°C. The scattering angle was set to 175° with the wavelength and filters set to automatic, and the samples were diluted as necessary for successful particle size measurements. All measurements were recorded in duplicate, and the average values and standard deviations are reported.

ACKNOWLEDGMENTS

The authors acknowledge funding from Strategic and Environmental Research and Development Program (WP-1381). We also thank the University of Dayton Dean's Summer Fellowship, Honor's program, and Chemistry Department for supporting JM and AS and UD Faculty Startup Funds for RKP. The authors acknowledge the National Science Foundation (CHE-2018678) for an MRI award and the Ohio Action Fund for leveraged support of the MRI award for the acquisition of a 400 MHz NMR spectrometer at the University of Dayton.

DATA AVAILABILITY STATEMENT

The data that support the findings of this study are available from the corresponding author upon reasonable request.

ORCID

Mark B. Masthay https://orcid.org/0000-0003-2091-9383

Justin C. Biffinger https://orcid.org/0000-0002-7330-9186

REFERENCES

[1] M. Baranska, J. C. Dobrowolski, G. Zajac, *Carotenoids: Nutrition, Analysis and Technology*, John Wiley & Sons **2016**.

[2] a) W. Horspool, F. Lenci, in *CRC Handbook of Organic Photochemistry and Photobiology*, 2nd ed. (Eds: W. Horspool, F. Lenci) Vol. 2004, CRC Press **2004**; b) A. Vershinin, *Biofactors* **1999**, *10*, 99. https://doi.org/10.1002/biof.5520100203

[3] S. Kumari, A. Goyal, M. Garg, *J. Nat. Prod.* **2021**, *11*, 617. https://doi.org/10.2174/2210315510999200806154609

[4] Q. P. Wang, C. Zhang, Y. H. Long, X. M. Wu, Y. Su, Y. Lei, Q. Ai, *Antibiotics-Basel* **2021**, *10*. https://doi.org/10.3390/antibiotics10030289

[5] T. J. Bunning, L. V. Natarajan, M. G. Schmitt, B. L. Epling, R. L. Crane, *Appl. Optics* **1991**, *30*, 4341. https://doi.org/10.1364/ao.30.004341

[6] Y. Sonoda, *J. Fluoresc.* **2022**, *32*, 95. https://doi.org/10.1007/s10895-021-02824-y

[7] V. Shesham, A. L. Kelly, W. Burke, A. Crouch, C. A. Drake, V. A. Varaljay, W. J. Crookes-Goodson, D. E. Barlow, M. B. Masthay, J. C. Biffinger, *J. Appl. Microbiol.* **2022**, *132*, 351. https://doi.org/10.1111/jam.15228

[8] A. Wassermann, *J. Chem. Soc.* **1959**, 986. https://doi.org/10.1039/jr9590000986

[9] a) B. F. Lutnaes, G. Kildahl-Andersen, J. Krane, S. Liaaen-Jensen, *J. Am. Chem. Soc.* **2004**, *126*, 8981. https://doi.org/10.1021/ja0492541 b) G. Kildahl-Andersen, L. Bruas, B. F. Lutnaes, S. Liaaen-Jensen, *Org. Biomol. Chem.* **2004**, *2*, 2496. https://doi.org/10.1039/b406913g c) B. F. Lutnaes, L. Bruas, G. Kildahl-Andersen, J. Krane, S. Liaaen-Jensen, *Org. Biomol. Chem.* **2003**, *1*, 4064. https://doi.org/10.1039/b307531a

[10] G. Kildahl-Andersen, S. N. Naess, P. B. Aslaksen, T. Anthonsena, S. Liaaen-Jensen, *Org. Biomol. Chem.* **2007**, *5*, 3027. https://doi.org/10.1039/b709535j

[11] a) S. Liaaen-Jensen, G. Kildahl-Andersen, *Arkivoc* **2008**, 5. https://doi.org/10.3998/ark.5550190.0009.602; b) J. Catalan, J. L. G. de Paz, *J. Chem. Phys.* **2006**, *124*. PMID: 10.1063/1.2158992; c) A. Mortensen, L. H. Skibsted, *J. Agric. Food Chem.* **2000**, *48*, 279. https://doi.org/10.1021/jf9904620; d) G. Thiele, A. Streitwieser, *J. Am. Chem. Soc.* **1994**, *116*, 446. https://doi.org/10.1021/ja00081a004 e J. S. Horwitz, R. A. Goldbeck, D. S. Kliger, *Chem. Phys. Lett.* **1981**, *80*, 229. https://doi.org/10.1016/0009-2614(81)80098-x

[12] K. H, H. Pelster, *Angew Chem - German* **1961**, *73*, 342.

[13] T. S. Sorensen, *J. Am. Chem. Soc.* **1965**, *87*, 5075. https://doi.org/10.1021/ja00950a017

[14] M. J. Frisch, G. W. Trucks, H. B. Schlegel, G. E. Scuseria, M. A. Robb, J. R. Cheeseman, G. Scalmani, V. Barone, G. A. Petersson, H. Nakatsuji, X. Li, M. Caricato, A. V. Marenich, J. Bloino, B. G. Janesko, R. Gomperts, B. Mennucci, H. P. Hratchian, J. V. Ortiz, A. F. Izmaylov, J. L. Sonnenberg, F. D. Williams, F. Lipparini, F. Egidi, J. Goings, B. Peng, A. Petrone, T. Henderson, D. Ranasinghe, V. G. Zakrzewski, J. Gao, N. Rega, G. Zheng, W. Liang, M. Hada, M. Ehara, K. Toyota, R. Fukuda, J. Hasegawa, M. Ishida, T. Nakajima, Y. Honda, O. Kitao, H. Nakai, T. Vreven, K. Throssell, J. A. Montgomery Jr., J. E. Peralta, F. Ogliaro, M. J. Bearpark, J. J. Heyd, E. N. Brothers, K. N. Kudin, V. N. Staroverov, T. A. Keith, R. Kobayashi, J. Normand, K. Raghavachari, A. P. Rendell, J. C. Burant, S. S. Iyengar, J. Tomasi, M. Cossi, J. M. Millam, M. Klene, C. Adamo, R. Cammi, J. W. Ochterski, R. L. Martin, K. Morokuma, O. Farkas, J. B. Foresman, D. J. Fox, Wallingford, CT, **2016**.

[15] R. Dennington, T. A. Keith, J. M. Millam, *GaussView, Version 6.1*, Semichem Inc, Shawnee Mission, KS **2016**.

[16] J. W. Ochterski, https://gaussian.com/thermo/, **2000**.

[17] C. Amovilli, F. M. Floris, *J. Phys. Chem. A* **2015**, *119*, 5327. https://doi.org/10.1021/jp510072n

[18] M. Kumar, D. H. Busch, B. Subramaniam, W. H. Thompson, *J. Phys. Chem. A* **2014**, *118*, 5020. https://doi.org/10.1021/jp5037469

[19] a) J. E. Nordlander, K. D. Kotian, D. E. Raff II, G. F. Njoroge, J. J. Winemiller, *J. Am. Chem. Soc.* **1984**, *106*, 1427. https://doi.org/10.1021/ja00317a039; b) A. D. Allen, T. T. Tidwell, *J. Am. Chem. Soc.* **1982**, *104*, 3145. https://doi.org/10.1021/ja00375a034

[20] a) D. Farcasiu, G. Marino, C. S. Hsu, *J. Org. Chem.* **1994**, *59*, 163. https://doi.org/10.1021/jo00080a026; b) A. D. Allen, T. T. Tidwell, O. S. Tee, *J. Am. Chem. Soc.* **1993**, *115*, 10091-10096. https://doi.org/10.1021/ja00075a026

[21] V. V. Konovalov, L. D. Kispert, *J Chem Soc-Perkin Trans* **1999**, *2*, 901. https://doi.org/10.1039/a800551f

[22] A. Wassermann, *J Chem Soc (Resumed)* **1954**, 4329. https://doi.org/10.1039/JR9540004329

[23] A. Wassermann, *Mol. Phys.* **1959**, *2*, 226. https://doi.org/10.1080/00268975900100221

[24] M. Buchwald, W. P. Jencks, *Biochemistry* **1968**, *7*, 834. https://doi.org/10.1021/bi00842a042

[25] A. Wassermann, *Trans. Faraday Soc.* **1957**, *53*, 1029.

[26] F. D. Collins, *Nature* **1950**, *165*, 817. https://doi.org/10.1038/165817c0

[27] W. M. Schubert, B. Lamm, *J. Am. Chem. Soc.* **1966**, *88*, 120. https://doi.org/10.1021/ja00953a023

[28] a) P. Riesz, R. W. Taft Jr., R. H. Boyd, *J. Am. Chem. Soc.* **1957**, *79*, 3724. https://doi.org/10.1021/ja01571a032; b) J. B. Levy, R. W. Taft Jr., L. P. Hammett, *J. Am. Chem. Soc.* **1953**, *75*, 1253. https://doi.org/10.1021/ja01101a514; c) R. M. O'Ferrall, *Adv. Phys. Org. Chem.* **2010**, *44*, 19. https://doi.org/10.1016/S0065-3160(08)44002-9; d) H. Mayr, M. Patz, M. F. Gotta, A. R. Ofial, *Pure Appl. Chem.* **1998**, *70*, 1993. https://doi.org/10.1351/pac199870101993

[29] a) S. Winstein, P. E. Klinedinst Jr., G. C. Robinson, *J. Am. Chem. Soc.* **1961**, *83*, 885. https://doi.org/10.1021/ja01465a035; b) S. Winstein, G. C. Robinson, *J. Am. Chem. Soc.* **1958**, *80*, 169. https://doi.org/10.1021/ja01534a045

[30] a) F. Joo, E. Papp, A. Katho, *Top. Catal.* **1998**, *5*, 113. b) E. Bianchini, L. Pietrobon, L. Ronchin, C. Tortato, A. Vavasori, *Appl. Catal., A* **2019**, *570*, 130. https://doi.org/10.1016/j.apcata.2018.11.014

[31] G. Stork, A. W. Burgstahler, *J. Am. Chem. Soc.* **1955**, *77*, 5068. https://doi.org/10.1021/ja01624a038

[32] a) A. G. M. Barrett, T. K. Ma, T. Mies, *Synthesis-Stuttgart* **2019**, *51*, 67. https://doi.org/10.1055/s-0037-1610382; b) T. Fukuyama, G. Liu, *J. Am. Chem. Soc.* **1996**, *118*, 7426. https://doi.org/10.1021/JA961701S

[33] a) H. Takao, A. Wakabayashi, K. Takahashi, H. Imagawa, T. Sugihara, M. Nishizawa, *Tetrahedron Lett.* **2004**, *45*, 1079. https://doi.org/10.1016/j.tetlet.2003.11.060; b) M. Nishizawa, T. Kashima, M. Sakakibara, A. Wakabayashi, K. Takahashi, H. Takao, H. Imagawa, T. Sugihara, *Heterocycles* **2001**, *54*, 629. https://doi.org/10.3987/COM-00-S(I)103

[34] a) S. A. Snyder, A. M. Levinson, *Comprehensive Organic Synthesis*, 2nd ed., Vol.3, Elsevier B.V, **2014**, pp. 268-292; b) N. C. Deno, C. U. Pittman Jr., J. O. Turner, *J. Am. Chem. Soc.* **1965**, *87*, 2153. https://doi.org/10.1021/ja01088a012

[35] M. J. Little, N. Aubry, M.-E. Beaudoin, N. Goudreau, S. R. LaPlante, *J. Pharm. Biomed. Anal.* **2007**, *43*, 1324. https://doi.org/10.1016/j.jpba.2006.10.039

[36] a) D. J. Nelson, C. Brammer, R. Li, *Tetrahedron Lett.* **2009**, *50*, 6454. https://doi.org/10.1016/j.tetlet.2009.08.128; b) A. D. Allen, M. Rosenbaum, N. O. L. Seto, T. T. Tidwell, *J. Org. Chem.* **1982**, *47*, 4234. https://doi.org/10.1021/jo00143a011

[37] T. J. Mason, R. O. C. Norman, *J. Chem. Soc., Perkin Trans.* **1973**, *2*, 1840. https://doi.org/10.1039/P29730001840

SUPPORTING INFORMATION

Additional supporting information can be found online in the Supporting Information section at the end of this article.

How to cite this article: M. B. Masthay, J. B. McLean, A. L. Santos, R. K. Pirlo, J. C. Biffinger, *J Phys Org Chem* **2022**, e4412. https://doi.org/10.1002/poc.4412